Journal of Energy Research and Reviews

3(1): 1-24, 2019; Article no.JENRR.49702
ISSN: 2581-8368

Determination of Energy and Exergy of Syngas Produced from Air-steam Gasification of Wheat Straw in a Dual Distributor Fluidized Bed Gasifier

Yaning Zhang[1,2*], Abdel Ghaly[2], Sammy S. Sadaka[3] and Bingxi Li[1]

[1]School of Energy Science and Engineering, Harbin Institute of Technology, Harbin, China.
[2]Department of Process Engineering and Applied Science, Faculty of Engineering, Dalhousie University, Halifax, Nova Scotia, Canada.
[3]Department of Biological and Agricultural Engineering, Division of Agriculture, University of Arkansas - AR, USA.

Authors' contributions

This work was carried out in collaboration among all authors. All authors read and approved the final manuscript.

Article Information

DOI: 10.9734/JENRR/2019/v3i130089
Editor(s):
(1) Dr. Salisu Muhammad Lawan, Department of Electrical and Electronics Engineering, Kano University of Science and Technology (KUST), Wudil, Nigeria.
Reviewers:
(1) Dodo Juliet Dingtsen, University of Jos, Nigeria.
(2) Hiren B. Soni, P.G., Institute of Science and Technology for Advanced Studies and Research, India.
Complete Peer review History: http://www.sdiarticle3.com/review-history/49702

Original Research Article

Received 07 April 2019
Accepted 20 June 2019
Published 27 June 2019

ABSTRACT

The energy and exergy of syngas produced from air-steam gasification of wheat straw in a dual-distributor fluidized bed gasifier under different operating conditions were evaluated. Three fluidization velocities (0.35, 0.40 and 0.45 m/s), 3 steam flow rates (0.20, 0.25 and 0.30 kg/min) and 3 biomass: steam ratios (3.00, 4.00 and 5.00 kg/kg) were investigated. The energy values of CO, H_2, N_2, CO_2, CH_4, C_2H_4 and C_2H_6 varied within the ranges of 1627.09-4646.60, 1543.30-2896.11, 274.75-1742.86, 82.03-574.24, 3225.39-4931.40, 1493.35-3777.44 and 892.74-2319.72 kJ/kg fuel, respectively. The overall energy distribution was (CH_4 & CO & C_2H_4 & H_2)>C_2H_6>(N_2 & CO_2). The results showed that when the fluidization velocity (FV) was increased from 0.35 m/s to 0.45 m/s (28.57%), the total energy of syngas increased by 1.16-28.59% depending on the steam flow rate (SFR} and biomass: steam ratio (B:S) used. Increasing the SFR from 0.20 kg/min to 0.30 kg/min (50.00%) decreased the total energy of syngas by 27.23-62.35% depending on the FV and B:S used. Increasing the B:S from 3.00 kg/kg to 5.00 kg/kg (66.67%) decreased the total energy of

**Corresponding author: E-mail: abdel.ghaly@dal.ca;*

syngas by 11.86-37.33% depending on the FV and SFR used. The exergy values of CO, H_2, N_2, CO_2, CH_4, C_2H_4 and C_2H_6 were in the ranges of 1486.70-4224.40, 1183.82-2209.00, 60.26-677.26, 54.02-452.97, 2913.74-4448.38, 1404.76-3541.76 and 833.00-2156.42 kJ/kg fuel, respectively. The overall exergy distribution was (CH_4 & CO)>(C_2H_4 & H_2 & C_2H_6)>(N_2 &CO_2). When the FV was increased from 0.35 to 0.45 m/s(28.57%), the total exergy of syngas increased by 1.45-26.93% depending on the SFR and B:S used. Increasing the SFR from 0.20 kg/min to 0.30 kg/min (50.00%) decreased the total exergy of syngas by 26.78-63.26% depending on the FV and B:S used. Increasing the B:S from 3.00 kg/kg to 5.00 kg/kg (66.67%) decreased the total exergy of syngas by 10.32-36.07% depending on the FV and SFR used. The effect of SFR on the total energy and total exergy of syngas was the highest, followed by B:S and FV. The highest energy (20004.54 kJ/kg fuel) and exergy (16886.06 kJ/kg fuel) of syngas were obtained at the FV of 0.45 m/s, the SFR of 0.20 kg/min and the B:S of 3.00 kg/kg.

Keywords: Energy; exergy; syngas; air; steam; gasification; wheat straw; fluidization velocity; biomass ratio; seam flow.

1. INTRODUCTION

Biomass materials such as cereal straws, rice husk, corn stalks, cotton stalks and wood residues have been used as the main energy source for thousands of years. Currently, biomass ranks the fourth source of energy in the world after oil, coal and natural gas and remains the main energy resource for heating and cooking in rural agricultural areas in many parts of the world [1]. Compared with coal and natural gas, biomass materials are renewable, accessible and less costly for many people all over the world [2].

Biomass materials can be used as an energy source in biochemical (biogas, bioethanol, biodiesel biohydrogen) and thermochemical (gasification, combustion and pyrolysis) conversion processes. However, thermochemical methods are much faster, have higher efficiencies, less costly and less selective of feed stocks [3,4]. Among the thermochemical conversion processes, gasification offers a high flexibility in using different biomass materials as well as in the generation of different products. In principal, all types of biomass can be converted by gasification into syngas comprising CO, CH_4, H_2, N_2, CO_2, H_2O and some hydrocarbons such as C_2H_4 and C_2H_6 [2,5]. This syngas can be used to provide various kinds of energy (heat, power) and chemical products [2]. The advantages of biomass gasification include: (a) minimum waste products, (b) lower gas emissions, (c) higher recycling rates and (d) higher efficiencies [5-7].

Gasification of biomass is performed by partial oxidation of the carbon contained in the biomass at high temperatures using a controlled amount of an oxidant which can be air, oxygen or steam [2]. Nipattummakul et al. [8] and Franco et al. [9] reported that the use of steam is more economical and results in higher hydrogen yield compared to other oxidants. Umeki et al. [10] and Wei et al. [11] reported that the water-gas shift reaction, which is vital for hydrogen production, could be enhanced by steam gasification leading to significantly higher heating values of syngas as a result of higher hydrogen production. Parthasarathy and Narayanan [3] reported heating values of syngas from gasification with air, oxygen and steam in the ranges of 4-6 MJ/m^3, 10-15 MJ/m^3 and 15-20 MJ/m^3, respectively.

Energy and exergy are important tools for evaluating energy sources and energy conversion technologies. The energy content of an object is an important property and can be converted to different forms such as work and heat but cannot be created or destroyed. The exergy is a measure of how a certain material deviate from the state of equilibrium with the environment and is defined as the maximum useful work possible during a process that brings the system into equilibrium with the environment. In contrast to energy, exergy can be destroyed when a process involves a temperature change [12,13].

The main objectives of this study were: (a) to determine the energy and exergy of the syngas produced from air-steam gasification of wheat straw in a dual-distributor type fluidized bed gasifier at various fluidization velocities (0.35, 0.40 and 0.45 m/s), steam flow rates (0.20, 0.25 and 0.30 kg/min) and biomass: steam ratios (3.00, 4.00 and 5.00 kg/kg) and (b) to detail the distributions of energy and exergy of syngas at these operating conditions.

2. ENERGY AND EXERGY OF SYNGAS

2.1 Energy of Syngas

The total energy of a gas stream can be written as the sum of its various energy as follows [14]:

$$En = En_{ki} + En_{po} + En_{ph} + En_{ch} \quad (1)$$

Where:

- En is the total energy of the gas stream (kJ/kg)
- En_{ki} is the kinetic energy of the gas stream (kJ/kg)
- En_{po} is the potential energy of the gas stream (kJ/kg)
- En_{ph} is the physical (sensible) energy of the gas stream (kJ/kg)
- En_{ch} is the chemical energy of the gas stream (kJ/kg)

Zhang [15] reported that the kinetic energy and potential energy represent very small portions (0.000001-0.0003% and 0.00002-0.003%, respectively) of the total energy of a gas and can be neglected. Thus, equation (1) can be simplified as follows:

$$En = En_{ph} + En_{ch} \quad (2)$$

The syngas generated from biomass gasification is a mixture of H_2, CO, CO_2, CH_4, C_2H_4, C_2H_6, N_2 and O_2. The physical energy of a syngas can be calculated from the following linear mixing equation [16].

$$En_{ph} = \sum_i n_i h_i \quad (3)$$

Where:

- n_i is the molar yield of the gas component i (mol/kg).
- h_i is the specific enthalpy of the gas component i (kJ/kmol).

Based on the specific enthalpy of gases at the environmental state specified in Table 1 (temperature T_0 = 25°C and pressure P_0 = 1 atm), the specific enthalpy of gases at an arbitrary temperature can be obtained from the following equation [17]:

$$h = h_0 + \int_{T_0}^{T} c_p \mathrm{d}T \quad (4)$$

Where:

- h is the specific enthalpy of the gas component at the arbitrary temperature (kJ/kmol).
- h_0 is the specific enthalpy of the gas at the environmental state (kJ/kmol).
- T_0 is the environmental temperature (298.15 K).
- T is the temperature of the gas under the arbitrary condition (K).
- c_p is the constant pressure specific heat capacity (kJ/kmol K).

The empirical equation of the constant pressure specific heat capacity is written as follows [17]:

$$\overline{c_p} = a + bT + cT^2 + dT^3 \quad (5)$$

Where:

- a,b,c,d are the coefficients of the constant pressure specific heat capacity (Table 2).

The chemical energy of a syngas is expressed as follows [14]:

$$En_{ch} = \sum_i n_i HHV_i \quad (6)$$

Where:

- HHV_i is the higher heating value of the gas component i (kJ/kmol)

2.2 Exergy of Syngas

The total exergy of a gas stream can be written as the sum of its various exergy as follows [20]:

$$Ex = Ex_{ki} + Ex_{po} + Ex_{ph} + Ex_{ch} \quad (7)$$

Where:

- Ex is the total exergy of the gas stream (kJ/kg)
- Ex_{ki} is the kinetic exergy of the gas stream (kJ/kg)
- Ex_{po} is the potential exergy of the gas stream (kJ/kg)
- Ex_{ph} is the physical exergy of the gas stream (kJ/kg)
- Ex_{ch} is the chemical exergy of the gas stream (kJ/kg)

Table 1. Higher heating value (HHV), chemical exergy (ex_{ch}), specific enthalpy (h_0) and specific entropy (s_0) of some gases at standard temperature and pressure (25°C and 1 atm)

Gas	HHV (kJ/kmol)[a]	ex_{ch} (kJ/kmol)[b]	h_0 (kJ/kmol)[a]	s_0 (kJ/kmol K)[a]
N_2	0	720	8669	191.502
O_2	0	3970	8682	205.033
H_2	285840	236100	8468	130.574
CO	282990	275100	8669	197.543
CO_2	0	19870	9364	213.685
CH_4	890360	831650	—	—
C_2H_4	1408400	1361100	—	—
C_2H_6	1556100	1495840	—	—

[a] *Cengel and Boles [18];* [B] *Moran et al. [19]*

Table 2. Coefficients of the constant pressure specific heat capacity of some gases [18]

Gas	*a*	*b* (×10^{-2})	*C* (×10^{-5})	*D* (×10^{-9})	Temperature range (K)
N_2	28.90	–0.157	0.808	–2.873	273–1800
O_2	25.48	1.520	–0.716	1.312	273–1800
H_2	29.11	–0.192	0.400	–0.870	273–1800
CO	28.16	0.168	0.533	–2.222	273–1800
CO_2	22.26	5.981	–3.501	7.469	273–1800
CH_4	19.89	5.024	1.269	–11.010	273–1500
C_2H_4	3.95	15.640	–8.344	17.670	273–1500
C_2H_6	6.90	17.270	–6.406	7.285	273–1500

Zhang [15] reported that the kinetic exergy and potential exergy represent very small portions (0.000002-0.007% and 0.00002-0.009%, respectively) of the total exergy of the gas and can be neglected. Thus, equation (7) can then be simplified as follows:

$$Ex = Ex_{ph} + Ex_{ch} \tag{8}$$

The physical exergy of syngas is calculated as follows [21]

$$Ex_{ph} = \sum_i n_i \left[(h - h_o) - T_o(s - s_o)\right] \tag{9}$$

Where:

- s is the specific entropy of the gas component *i* at the arbitrary temperature (kJ/kmol K)
- s_0 is the specific entropy of gas the component *i* at the environmental state (kJ/kmol K)

Based on the specific enthalpy of N_2, O_2, H_2, CO, CO_2, CH_4, C_2H_4 and C_2H_6 at the environmental state shown in Table 1, the specific entropy of the gases at the arbitrary temperature can also be obtained as follows [17]:

$$s = s_0 + \int_{T_0}^{T} \frac{c_p}{T} dT - R \ln \frac{P}{P_0} \tag{10}$$

Where:

- R is the universal gas constant (8.314472 kJ/kmol K)
- P is the pressure of the gas component *i* at the arbitrary state (Pa)
- P_0 is the pressure of the gas component *i* at the environmental state (Pa)

The chemical exergy of syngas is calculated as follows [21]:

$$Ex_{ch} = \sum_i n_i \left(ex_{ich} + RT_o \ln \frac{n_i}{\sum n_i}\right) \tag{11}$$

Where:

- ex_{ich} is the standard chemical exergy of the gas component *i* as shown in Table 1 (kJ/kmol)

3. EXPERIMENTAL MATERIALS

3.1 Wheat Straw

Winter wheat straw (Max) was collected in the form of small rectangular bales (46 cm × 48 cm × 70 cm) from a field located in Dyke View Farms Limited, Port Williams, Nova Scotia, Canada. In order to obtain consistent moisture content of the feedstock, the straw bales were dried in a

specially designed bale drying unit to a moisture content of 10±1%. Bales of dried straw were chopped using a specially designed straw chopper Ghaly et al. [22] to an average size of 1.5×2×0.3 mm. Some properties of the chopped straw are given in Table 3.

3.2 Bed Materials

Alumina sand was used as inert bed material in the fluidized bed gasifier. It was obtained from Diamonite Products Limited, Shreve, Ohio, USA. The alumina sand was kiln fired at 1500^{o}C and the sand particles were very spherical in shape. The main characteristics and chemical composition of the alumina sand are given in Table 4.

4. EXPERIMENTAL APPARATUS

Fig. 1 shows a schematic of the gasification system used in this study. It consisted of a dual distributor fluidized bed gasifier, a steam generation system, a gas sampling system and a computer and data acquisition system.

Table 3. Some characteristics of wheat straw

Characteristics	Value	Unit
Moisture content	10±1	%
Average particle size	1.5×2×0.3	mm
Bulk density	75-80	kg/m^3
Lower heating value	18.71	MJ/kg
Proximate analysis [a]		
Volatile matter	77.80	%
Fixed carbon	17.61	%
Ash	3.59	%
Ultimate analysis [a]		
C	45.97	%
H	5.78	%
O	44.15	%
N	0.55	%
S	0.12	%
Cl	0.05	%
Ash	3.41	%

[a] *Weight percentage on dry basis*

Table 4. Some characteristics of the alumina sand

Characteristics	Value	Unit
Particle density	3450	kg/m^3
Bulk density	2000	kg/m^3
Maximum particle size	500	µm
Mean particle size	380	µm
Minimum particle size	300	µm
Minimum fluidization velocity [a]	0.15	m/s
Chemical composition		
Alumina (Al_2O_3)	85.0-90.0	%
Silica (SiO_2)	8.0-10.0	%
Calcia (CaO)	0.5-2.0	%
Magnesia (MgO)	0.5-1.5	%
Soda (Na_2O)	0.1-0.4	%
Iron Oxide (Fe_2O_3)	0.1-0.3	%
Titania (TiO_2)	0.05-0.15	%
Potasia (K_2O)	0.01-0.05	%

[a] *Calculated for ambient conditions*

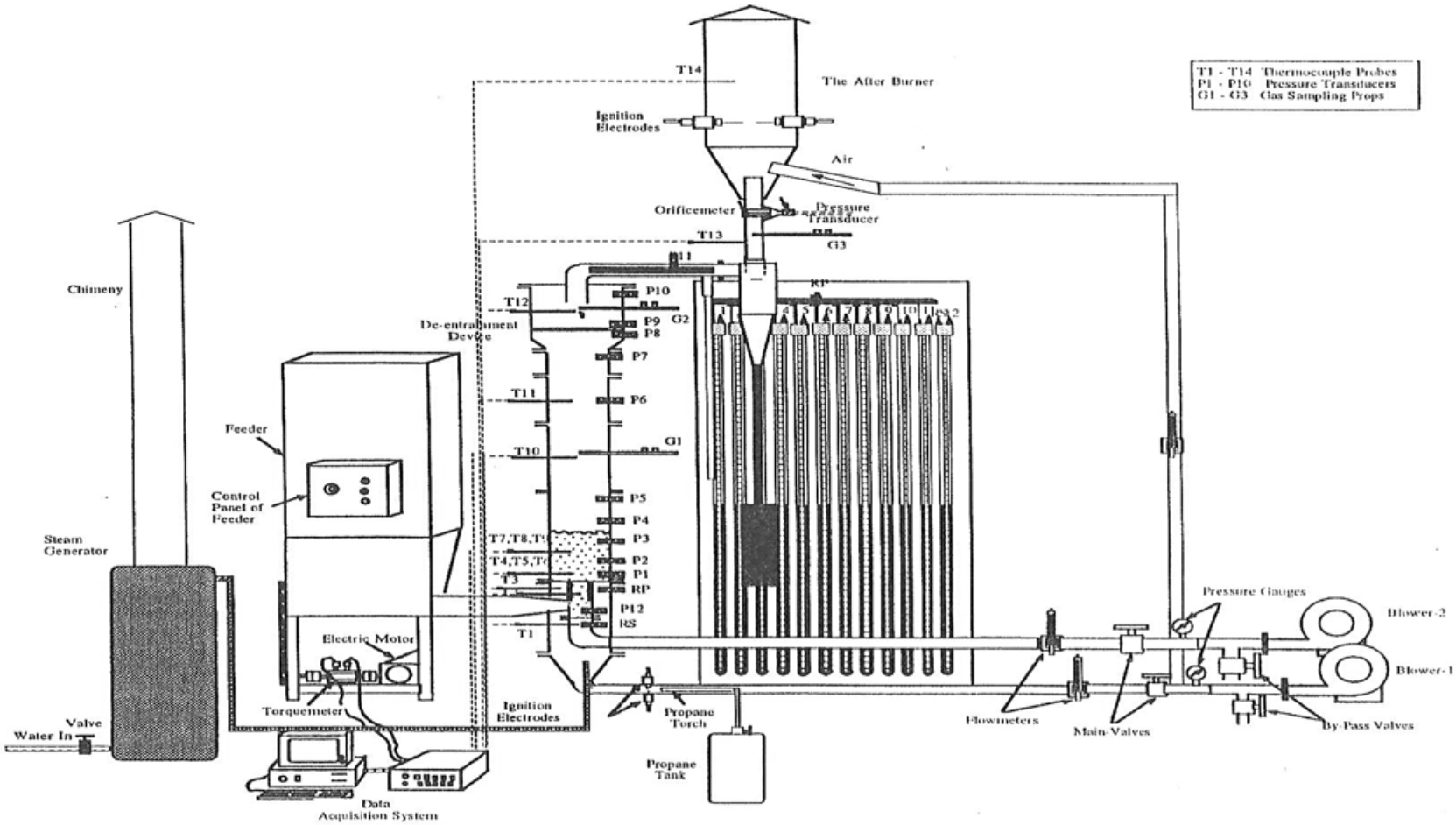

Fig. 1. The experimental apparatus

4.1 The Dual-Distributor Fluidized Bed Gasifier

The dual distributor fluidized bed gasifier is a further development of a spout-fluidized gasifier bed in which a bubbling fluidized bed is maintained towards the outer region of the bed while the active spout is maintained at the center. It has a secondary distributor plate in the spout region above the secondary column. The biomass material is fed into the secondary column by specially designed straw feeder by Ghaly et al. [23]. By the virtue of its design, the dual distributor fluidized bed ensures a more homogeneous mixture of biomass and bed materials since the biomass is pneumatically introduced through the bottom center of the reactor by the secondary column. The uniform biomass distribution in the dual distributor fluidized bed is assured by the spout which entrains the bed particles from the bottom of the bed, mix them with biomass particles and secondary air and then transport the mixture into the upper region of the bed. From here, the bed particles and the un-reacted biomass material proceed in a three-dimensional fashion and their directions are determined by the movement of bubbles in the bed. The systematic pattern of solids movement gives rise to a unique hydrodynamic system which is more suitable for the gasification of low-density biomass materials. The dual distributor fluidized bed gasifier used in the study consisted of an air supply system, start-up system, a fluidizing column with a feeding mechanism, a disengagement section with a de-entrainment device, a cyclone and an after burner.

The air supply system was used to provide the primary air (for fluidization) and secondary air (for biomass feeding) as well as the air required for the afterburner. Each air supply consisted of a blower, a pressure gauge having a pressure range of 0-690 kPa, a main valve to control the flow rate, a by-pass valve to prevent overheating of the electric motor, a steel pipe having an inner diameter of 50 mm and a flowmeter. The blower (Model ENGENAIR R4310A-2, Benton Harbour, Michigan, USA) was driven by a 4.8 hp (three-phase 220 volts and 13.4 amps) electric motor (Baldor Industrial Motor, Benton Harbour, Michigan, USA) and had a maximum flow capacity of 4.87 m^3/min and maximum pressure of 20 kPa. The blower inlet had a filter with a micron rating of 25 and a maximum flow of 7.08 m^3/min to clean the incoming gas of contaminants such as dust particles and water. Flow Cell Bypass flowmeters (Metal FLT-type, Cat. No. N-03251-60, Cole Parrnar, Chicago, Illinois, USA) were used to measure the air supply rates. Each flowmeter was accurate to 2.5% of full scale and could be used up to maximum temperature and pressure of 60^{o}C and 1035 kPa, respectively.

The start-up system consisted of a propane tank, a pressure regulator, a solenoid valve, a gas flowmeter. A safety mechanism was incorporated into the unit to ensure that no propane was supplied to the system unless both the air supply system and the ignition system were on. This mechanism was made of solenoid valve (Model No. CG8215-G10, Honeywell, Mississauga, Ontario, Canada) connected to the control panel. The air was detected through a pressure tap connected to a pressure switch (Model No. C645, Honeywell, Mississauga, Ontario, Canada) The flame was detected by an ultraviolet detector (Model No. C7027 A, Honeywell, Mississauga, Ontario, Canada). To raise the temperature of the reactor to the required level, a start-up period was required to heat the fluidized bed to the ignition temperature of the straw using the propane.

The fluidized bed gasifier was made of 8 mm thick, 310 stainless steel cylinder of 255 mm diameter and 2700 mm height. A dual distributor plate type feeding mechanism was used to feed the straw. The system (Fig. 2) consisted of the lower portion of the main column (the wind box and conical inlet section) which is connected the main air stream supply, the secondary column which is connected to the secondary air supply, the secondary distributor plate and the end piece of the augur casing of the feeding unit. The primary air supply line was connected to the conical inlet section which was made of 4 mm thick 310 stainless steel. A 0.5 m tall circular section made of 310 stainless steel pipe of 8 mm thickness was added on the top of the conical inlet section and acted as a wind box. A 40 mm diameter port was provided near the bottom of the bed to remove the bed material. The fluidization column was insulated using a flexible blanket (Inswool-HP Blanket, A. P. Green Industries Inc., New Mexico, Missouri, USA) to reduce heat loss from the system.

An enlarged disengagement section was mounted on the top of the main fluidization column and used to reduce the elutriation rate from the fluidized bed. It was made of 4 mm thick hot rolled steel. The height of the enlarged

section was 395 mm whereas the bottom and top diameters were 255 and 355 mm, respectively. The angle of inclination was 30^{o} from the vertical axis. The top of the enlarged section was covered by 8 mm thick 310 stainless steel plate. A pipe made of 6 mm thick stainless steel with a cross section of 80 mm by 40 mm was connected to the top of the enlarged section and used as a gas outlet to the gasifier and gas inlet to the cyclone. A de-entrainment device (Fig. 3) was placed inside the disengagement section. It consisted of 16 triangular blades made of 310 stainless steel and inclined 300 to the horizontal. The distance from the top of the blade to the overlapping one was 61 mm. The diameter of the structure was 344.4 mm giving a clearance of 5.6 mm between the device and the wall of the disengagement section. The total open area of the structure on the horizontal plane was 714 mm. The enlarged section was insulated using a flexible blanket (Inswool-HP Blanket, A. P. Green Industries Inc., New Mexico, Missouri, USA) to reduce heat loss from the system.

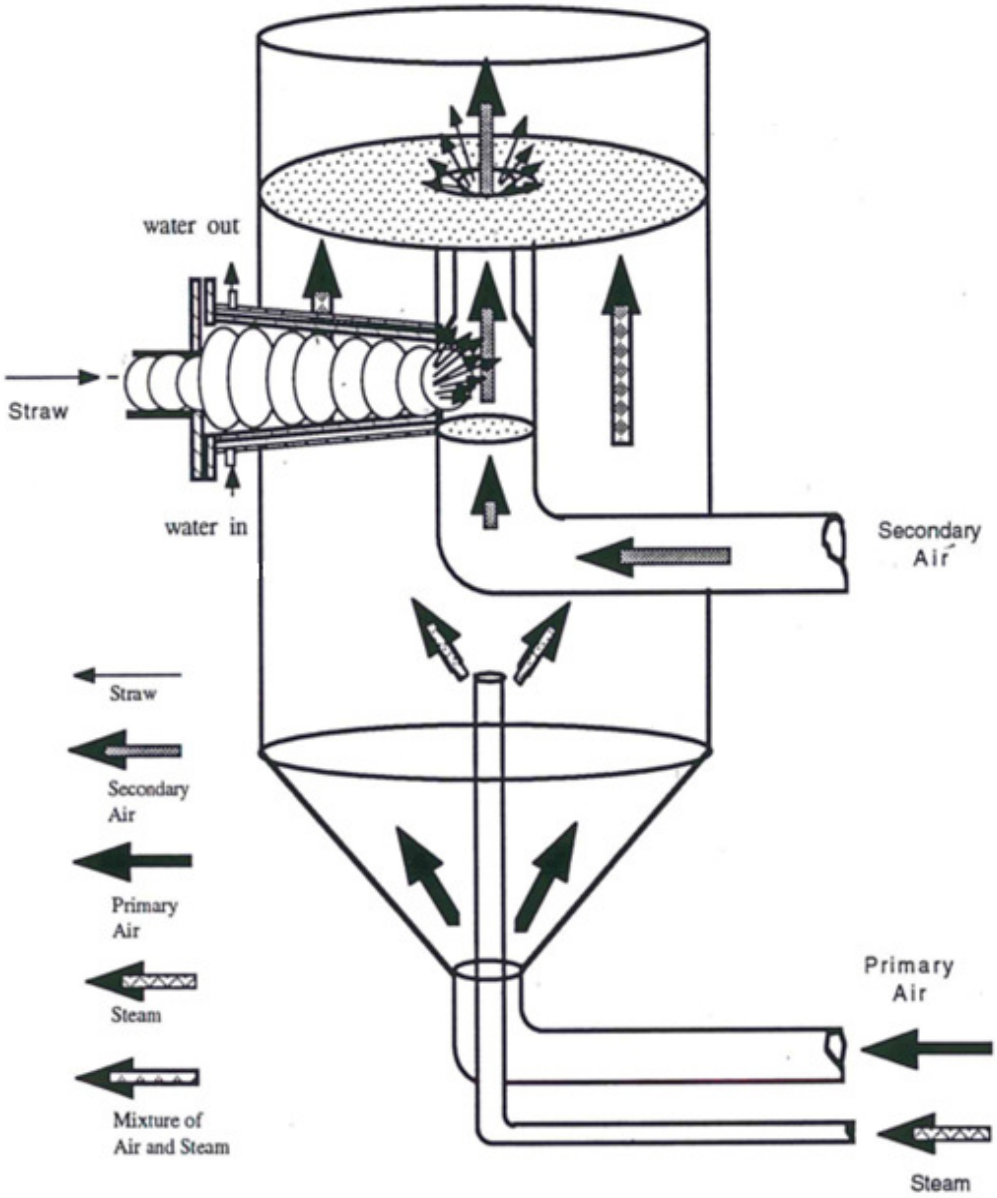

Fig. 2. The air supplies and feeding mechanism

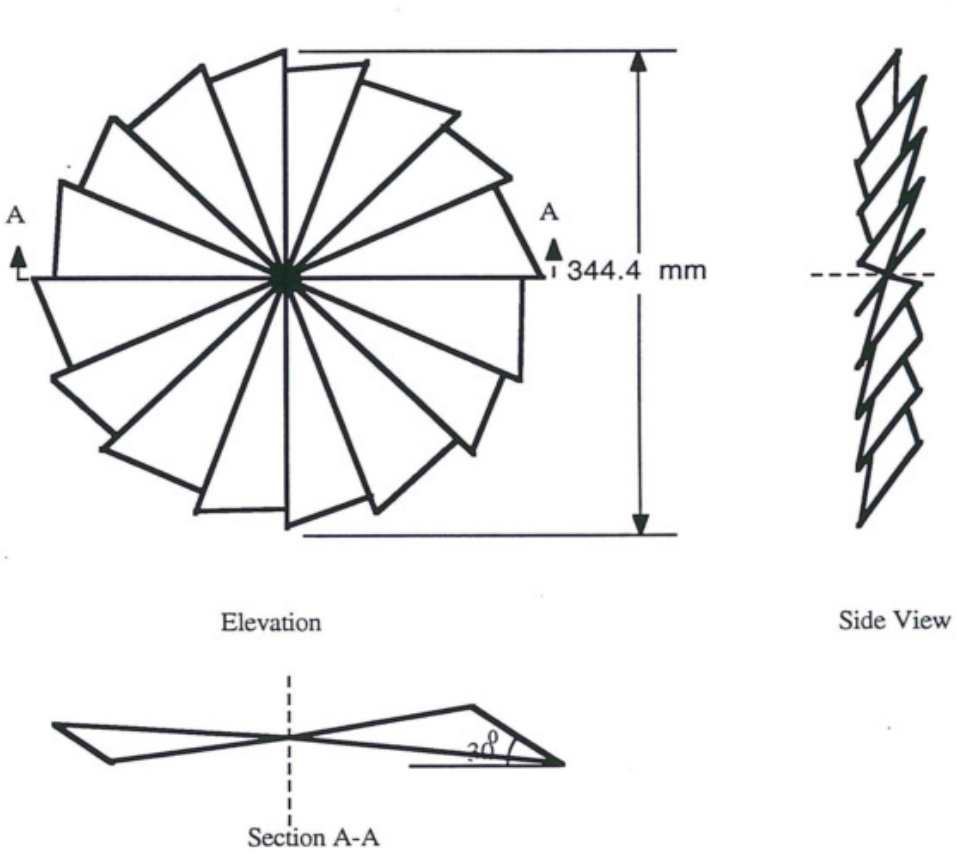

Fig. 3. The de-entrainment device

A cyclone was connected to the exit of the disengagement section to capture the solid particles (dust, ash and char) escaping from the bed. The cyclone had a conical section of 38 mm small diameter and 300 mm length and cylindrical section of 159 mm diameter and 300 mm length. The gas leaves the cyclone through a stainless-steel pipe of 150 mm inside diameter to the combustion chamber of the afterburner. The captured particles were collected in the solid particles collector which was attached to the bottom of the cyclone. The cyclone was insulated using a flexible blanket (Inswool-HP Blanket, A. P. Green Industries Inc., New Mexico, Missouri, USA) to reduce heat loss from the system.

The afterburner consisted of two ignition electrodes, an air supply unit, a mixing chamber, a combustion chamber and an exhaust duct. The combustion chamber was constructed from stainless steel and has a diameter of 500 mm and a height of 2000 mm. The exhaust duct was housed inside a pipe of 500 mm diameter for safety. The air is piped to the combustion chamber through 4 pipes of 6 cm inside diameter and 15º angle on the horizontal. The main air pipe has a damper for air flow regulation an air flow meter. The produced gas entered from the bottom through the 150 mm diameter pipe and the air entered from the 4 pipes at the end of this pipe.

4.2 Steam Supplying System

A steam generator (Model No. MHPH 330 Easy Kleen Company, Sussex, New Brunswick, Canada) was used to generate the steam which was mixed with air in the main column of the gasifier. The steam generator (Fig. 4) had a maximum output of 0.022 m^3/min of steam at a temperature of 170ºC. The water heater coils were designed to operate safely at working pressure of up to 20.68 MPa. A hose with a regulator was used to connect the steam generator to the main propane line. The input energy required for the steam generator was 348.17 MJ. A heavy duty steam hose was used to connect the steam generator to the main column of the gasifier. A water flow meter was fixed into the water pipe and used to adjust the

water flow rate to the steam generator. The steam generator was designed to turn on and off the flame at the pre-adjusted steam temperature. A calibration was made to adjust the propane flow rate at the corresponding water flow rate to maintain constant steam temperature.

4.3 Gas Sampling System

The gas sampling (Fig. 5) system used in this study consisted of a gas sampling probe, copper tubing, a three-way switch valve, a gas purifier, a compressed air line, a peristaltic pump, a sampling bulb, a pressure relief valve, a pressure gauge, a syringe and evacuated tubes. Stainless steel gas sampling probes (each with a cooling jacket) were designed and manufactured. Each probe was 1.27 cm in diameter and 45.5 cm in length. The diameter of the sampling tube placed inside the probe was 0.64 cm. The gas sampling probe was located at the exit of the cyclone. A peristaltic pump (MasterFlex Cat. No. N-07567-70, Cole Palmer, Chicago, Illinois, USA) was used to draw the gas from the gasifier and compress it into the gas sampling bulb. To remove moisture, tar and other impurities from the gas, a gas purifier (Cat. No. N-01418-50, Cole Palmer, Chicago, Illinois, USA) was placed between the gas sampling bulb and the peristaltic pump. The gas sampling bulbs (Cat. No. N-06650-40, Cole Palmer, Chicago, Illinois, USA) could store 0.25 L of gas sample at a maximum gauge pressure of 100 kPa. In order to maintain the gas pressure at the desired level inside the gas sampling bulbs, an adjustable relief valve (Cat. No. SS-4-CPA-3, Nupro Company, Willoughby, Ohio, USA) and a pressure gauge having a pressure range of 0-200 kPa (P0121BP, Invensys Systems, Inc., Houston, Texas, USA) were mounted at the exit of each gas sampling bulbs. A syringe and evacuated tube assembly was used to collect the gas sample from the gas sampling bulb. Evacuated tubes having a volume of 10 mL each (Vacutainer. Model 6430, Becton Dickinson, Franklin Lakes, New Jersey, USA) were used to store the gas samples. These tubes were initially evacuated by the manufacturer up to 80% by volume. They were re-evacuated up to 98% by volume using a vacuum pump (Model RV5, Edwards, Albany, New York, USA) before being used. To remove the moisture, tar and other impurities from the gas, a gas purifier (Cat. No. N-01518-50 Cole Palmer, Chicago, Illinois, USA) was placed between the gas sampling bulb and the peristaltic pump.

4.4 Computer and Data Acquisition System

A microcomputer and a data acquisition system were used to record and display the measured temperature and flow rate values. An analog/digital conversion card (Cat. No. N-08109-25, Cole Parmer, Chicago, Illinois, USA) was used with two thermocouple Amplifier-Multiplexers (Cat. No. N-08109-00, Cole Parmer, Chicago, Illinois, USA), each can read up to six thermocouples with a resolution of ± 0.1^{o}C. The data logging software (Cat. No. N-08109-32, Cole Parmer, Chicago, Illinois, USA) which could read 16 inputs in one second was modified and used to display the temperature and feed rate values on the screen and store the data in the computer. Type K special purpose thermocouple probes (Cat No. N-08515-70, Coke Parmer, Chicago, Illinois, USA) with special color-coded mini connector plugs, having a temperature range of 200-1372ºC, were used to measure the gasifier temperatures in the dense bed and free board. The pressure drop was measured at different locations of the fluidized bed gasifier using Dwyer slack-tube manometer (Model No. 1211-200, Dwyer, Muxhigan City, Indiana, USA). Each manometer had a flexible vinyl-plastic column and a spring steel scale calibrated in centimeters of green colored water for a range of pressure readings of up to 200 cm of water. Each pressure tab on the gasifier was connected to a separate manometer via a flexible tygon tubing of 8 mm inside diameter. The other end of the manometer was connected to a reference point located 50 mm blow the main distribution plate through a manifold of 255 mm diameter.

5. EXPERIMENTAL PROCEDURE

5.1 Experimental Design

The effects of fluidization velocity (0.35, 0.40 and 0.45 m/s), steam flow rate (0.20, 0.25 and 0.30 kg/min) and biomass: steam ratio (3.00, 4.00 and 5.00 kg/kg) on the energy and exergy of syngas were investigated. The fluidization velocity (FV) was controlled by altering the primary air supply rate though the main distributor plate. The wheat straw feed rate (WSFR) was controlled by adjusting the auger of the straw feeder. The steam flow rate (SFR) and biomass: steam ratio (B:S) were controlled by altering the steam supply rate from the steam generator. The flow rates of feedstock and steam at various fluidization velocities are given in Table 5.

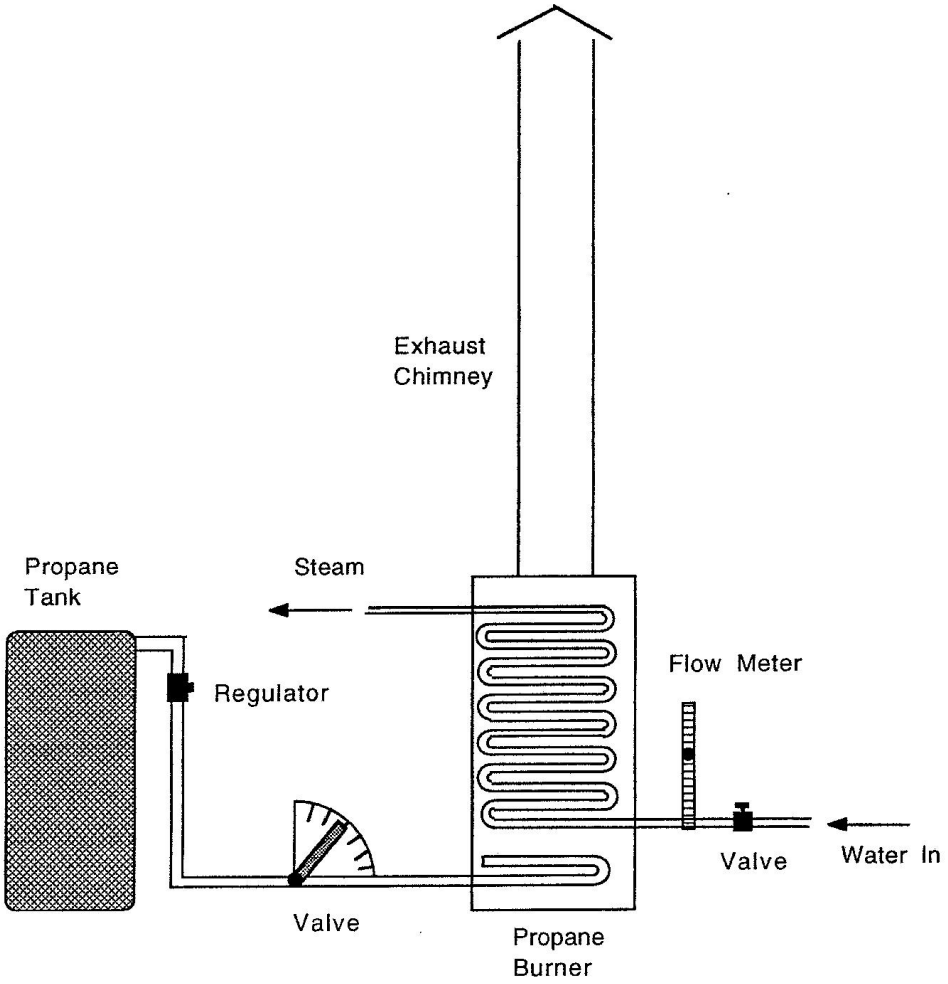

Fig. 4. The steam generation system

5.2 Experimental Protocol

An empty particle collector was attached to the bottom of the cyclone. Thermocouples were connected to the data logger. The water bath was switched on and the cooling line was started up. The primary air supply was turned on to fluidize the sand particles in the main fluidizing column and the air flow rate was adjusted to 0.56 kg/min. The master propane shut-off valve was opened and the main switch of the start-up unit was turned on. Both the pressure switch and the flame detector were reset. The manometers were connected to proper taps and zeroed. The start-up unit switch was turned on. The ignition electrodes and the solenoid valve were activated automatically after 30 s at the same time to supply and burn propane in the primary airline. The propane supply rate was adjusted to give a blue flame at the optimal air/fuel ratio. The temperature rose as a result of the heat released from the combustion of the propane–air mixture. Once the bed temperature reached 500°C, the start-up system was shut down and the straw was introduced into the bed by turning on the feeder while the primary air supply was kept on to cool the bottom section (wind box) of the gasifier. The bed temperature increased rapidly (to approximately 750°C) by the energy released from the combustion of straw in the fluidized bed. The inlet water flowmeter was adjusted to generate the proper amount of steam flow rate. The produced steam was drained until the steam temperature reached 150°C and then the valve was turned on to introduce the steam into the fluidized bed gasifier.

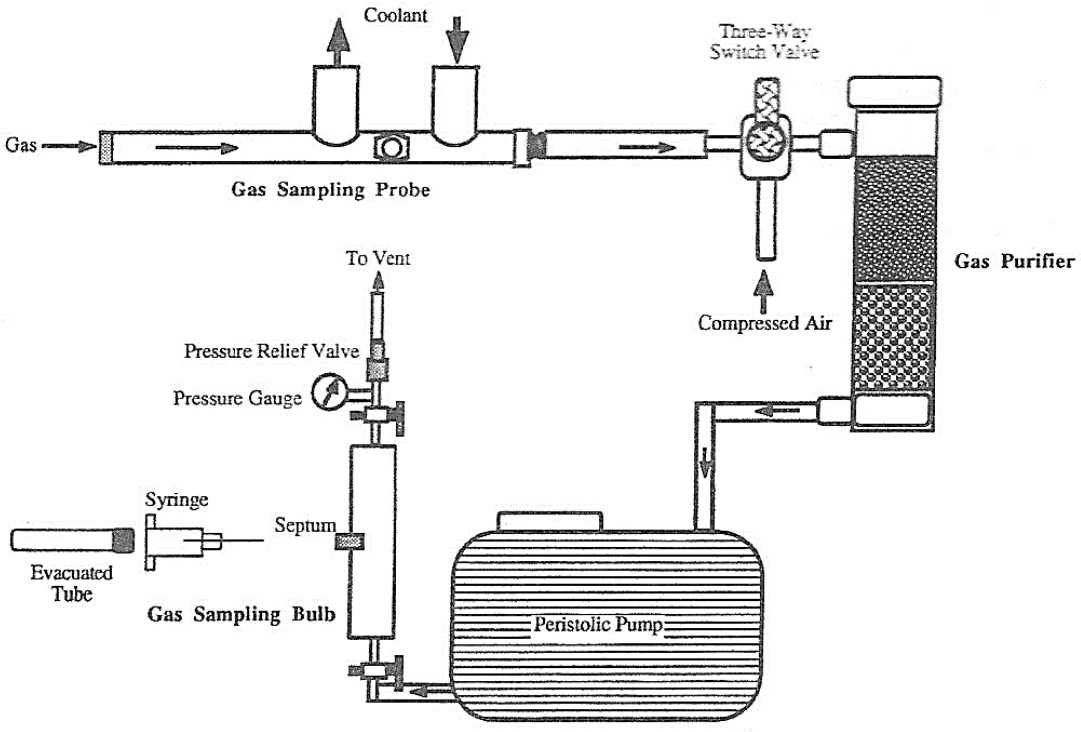

Fig. 5. Gas sampling system

The fuel feed rate, steam flow rate and air flow rates were adjusted to the desired respective levels. The system was operated at this condition for 50 min to ensure that the steady-state condition was reached in the fluidized bed reactor. Steady-state conditions were ensured from the constant temperature and produced gas flow rate. The microcomputer-based data acquisition system monitored and recorded the temperature and the feed rate values. The pressure drop across the orifice plate was recorded through the inclined manometer and the bed pressure drop data were recorded from the U-tube manometers. When sampling and data recording was completed the feeder, secondary air supply, steam supply and primary air supply were shut down in that order. The ash collector was replaced by an empty one. The same procedure was repeated for all the experiments.

5.3 Gas Sampling and Analysis

The gas sampling procedure was initiated by purging the line and the gas sampling probe with compressed air (550 kPa). Using the three-way switch valve, the gas sampling probe was disconnected from the compressed air line and connected to the sampling line. The peristaltic pump was turned on to draw the gas from the gasifier through the gas sampling probe and compress it into the gas sampling bulb. The valve at the exit of the sampling bulb was kept open for three minutes in order to flush the sampling bulb with fresh gas from the gasifier. The valve was closed and the sampling bulb was filled with the gas sample. The gas sample was collected in an evacuated tube using a syringe. The tube was kept in position for about one minute to allow it to be filled with the gas from the sampling bulb. All the gases were analysed using a gas chromatograph (Hewlett Packard Model 5890 Series II Gas Chromatograph, GMI, Inc., Ramsey, Minnesota, USA). Argon was used as the carrier gas, so as to be able to detect hydrogen besides the other gas components.

6. RESULTS AND DISCUSSION

The mean temperatures of the dense bed in the gasifier, gas components and high heating values measured at various fluidization velocities, steam flow rates and biomass: steam ratios are shown in Table 6.

Table 5. Flow rates of wheat straw and steam and the biomass: Steam ratio

FV (m/s)	WSFR (kg/min)	SFR (kg/min)	B:S (kg/kg)
0.35	0.60	0.20	3.00
	0.80	0.20	4.00
	1.00	0.20	5.00
	0.75	0.25	3.00
	1.00	0.25	4.00
	1.25	0.25	5.00
	0.90	0.30	3.00
	1.20	0.30	4.00
	1.50	0.30	5.00
0.40	0.60	0.20	3.00
	0.80	0.20	4.00
	1.00	0.20	5.00
	0.75	0.25	3.00
	1.00	0.25	4.00
	1.25	0.25	5.00
	0.90	0.30	3.00
	1.20	0.30	4.00
	1.50	0.30	5.00
0.45	0.60	0.20	3.00
	0.80	0.20	4.00
	1.00	0.20	5.00
	0.75	0.25	3.00
	1.00	0.25	4.00
	1.25	0.25	5.00
	0.90	0.30	3.00
	1.20	0.30	4.00
	1.50	0.30	5.00

FV = fluidization velocity; WSFR= wheat straw feed rate; SFR = steam flow rate; B:S = biomass to steam ratio

6.1 Mean Temperatures of the Bed

When the FV was increased from 0.35 to 0.45 m/s (28.57%), the mean temperature increased from 1077 to 1168 K (8.45%), from 1022 to 1151 K (12.62%), from 970 to 1089 K (12.27%) at the SFR of 0.20 kg/min and the B:S of 3.00, 4.00 and 5.00 kg/kg; from 1034 to 1167 K (12.86%), from 985 to 1112 K (12.89%), from 933 to 1065 K (14.15%) at the SFR of 0.25 kg/min and the B:S of 3.00, 4.00 and 5.00 kg/kg; and from 988 to 1109 K (12.25%), from 922 to 1036 K (12.36%) and from 882 to 992 K (12.47%) at the SFR of 0.30 kg/min and the B:S of 3.00, 4.00 and 5.00 kg/kg, respectively. The results obtained from this study showed that higher fluidization velocity achieved a better mixing of feed material with bed material and thus resulted in better heat transfer and higher temperature. Sharma et al. [24] that higher fluidization velocity can breakdown segregated lumps and result in a better particle mixing. Mansaray et al. [25] indicated that the increased fluidization velocity increased the rate of exothermic reactions and raised the temperature of the bed. Sadaka et al. [26] stated the heat released from the exothermic oxidation process was utilized to pyrolyze the increased biomass material which contributed to the reduction in the bed temperature.

However, when the SFR was increased from 0.20 to 0.30 kg/min (50.00%), the mean temperature decreased from 1077 to 988 K (9.01%), from 1022 to 922 K (10.85%), from 970 to 882 K (9.98%) at the FV of 0.35 m/s and the B:S of 3.00, 4.00 and 5.00 kg/kg; from 1154 to 1059 K (8.97%), from 1097 to 998 K (9.92%), from 1039 to 945 K (9.95%) at the FV of 0.40 m/s and the B:S of 3.00, 4.00 and 5.00 kg/kg; and from 1168 to 1109 K (5.32%), from 1151 to 1036 K (11.10%) and from 1089 to 992 K (9.78%) at the FV of 0.45 m/s and the B:S of 3.00, 4.00 and 5.00 kg/kg, respectively.

Table 6. Bed temperatures, gas compositions and HHVs

FV	SFR	B:S	T	Gas components (mol/kg)							HHV
(m/s)	(kg/min)	(kg/kg)	(K)	CO	H_2	N_2	CO_2	CH_4	C_2H_4	C_2H_6	(MJ/Nm^3)
0.35	0.20	3.00	1077	13.88	8.13	35.41	1.76	4.88	2.30	1.22	9.08
		4.00	1022	12.48	7.46	27.35	4.78	4.30	2.09	1.07	9.25
		5.00	970	11.66	6.86	21.73	6.86	4.08	2.07	1.09	9.63
	0.25	3.00	1034	10.44	7.00	25.49	7.29	5.25	1.75	0.93	9.22
		4.00	985	10.05	6.81	18.47	10.59	5.02	1.67	0.86	9.54
		5.00	933	9.30	6.41	14.97	10.76	4.55	1.71	0.93	9.94
	0.30	3.00	988	8.07	6.34	18.44	8.53	4.90	1.38	0.72	9.07
		4.00	922	6.45	5.77	12.50	8.00	4.14	1.07	0.56	9.69
		5.00	882	5.60	4.95	10.45	7.19	3.60	1.05	0.58	10.10
0.40	0.20	3.00	1154	14.25	8.68	41.32	1.83	4.94	2.47	1.27	8.01
		4.00	1097	13.04	7.34	31.51	4.53	4.53	2.13	1.17	8.32
		5.00	1039	12.22	6.70	25.38	6.33	4.22	1.99	1.05	8.53
	0.25	3.00	1111	11.13	7.67	29.72	6.85	4.95	1.90	1.02	8.15
		4.00	1054	10.49	7.35	21.76	9.70	4.70	1.69	0.90	8.60
		5.00	1013	9.61	6.68	18.13	10.75	4.34	1.57	0.81	8.78
	0.30	3.00	1059	6.49	6.03	23.35	6.85	4.29	1.33	0.72	8.01
		4.00	998	5.78	6.26	16.79	7.81	3.63	1.08	0.56	8.43
		5.00	945	5.23	5.58	13.28	8.05	3.46	1.02	0.55	8.57
0.45	0.20	3.00	1168	14.57	9.04	48.91	8.78	4.39	2.55	1.40	7.19
		4.00	1151	12.45	7.59	37.49	5.46	4.10	2.28	1.21	7.30
		5.00	1089	11.12	6.94	34.04	7.15	3.91	2.09	1.08	7.62
	0.25	3.00	1167	11.62	7.99	36.82	5.95	5.01	1.82	0.94	7.72
		4.00	1112	10.06	7.25	28.44	9.13	4.50	1.63	0.88	7.95
		5.00	1065	8.97	6.83	22.04	10.71	4.34	1.50	0.81	8.00
	0.30	3.00	1109	10.03	7.65	27.05	9.96	4.95	1.39	0.73	7.66
		4.00	1036	7.23	7.91	22.65	12.07	4.50	1.25	0.68	7.87
		5.00	992	6.64	7.43	17.44	13.70	4.32	1.21	0.63	8.09

FV= the fluidization velocity, SFR= steam flow rate, B:S= biomass: steam ratio, HHV= the higher heating value of syngas

Also, when the B:S was increased from 3.00 to 5.00 kg/kg (66.67%), the mean temperature decreased from 1077 to 970 K (11.03%), from 1034 to 933 K (10.83%), from 988 to 882 K (12.02%) at the FV of 0.35 m/s and the SFR of 0.20, 0.25 kg/min and of 0.30 kg/min; from 1154 to 1039 K (11.07%), from 1111 to 1013 K (9.67%), from 1059 to 945 K (12.06%) at the FV of 0.40 m/s and the SFR of 0.20, 0.25 and 0.30 kg/min; and from 1168 to 1089 K (7.25%), from 1167 to 1065 K (9.58%) and from 1109 to 992 K (11.79%) at the FV of 0.45 m/s and the SFR of 0.20, 0.25 and 0.30 kg/min, respectively.

6.2 Compositions of Syngas

The gas components CO, H_2, N_2, CO_2, CH_4, C_2H_4 and C_2H_6 varied within the ranges of 5.23-14.57, 4.95-9.04, 10.45-48.91, 1.76-13.70, 3.46-5.25, 1.02-2.55 and 0.55-1.40 mol/kg fuel, respectively.

The results showed that increasing the FV increased the yield of N_2 due to the increased air. However, the FV showed no obvious effects on the yields of the other component gases. Several researchers reported variations in the gas components as a result of changes in the FV. Mansaray et al. (1999) stated that increasing the FV increased the concentrations of N_2 and CO_2. Sadaka et al. [26] and Mansaray et al. [25] stated that increasing the FV could decrease the mole fractions of CO, H_2, CH_4, C_2H_4 and C_2H_6.

Generally, increasing the SFR decreased the yields of CO, H_2, N_2, C_2H_4 and C_2H_6 and initially increased the yield of CH_4 which then decreased with further increases in the SFR. However, the SFR showed no obvious effect on the yield of CO_2. Similar results were reported by Li et al. [27] for steam gasification of wood pellets.

The results also showed that increasing the B:S decreased the yields of CO, H_2, N_2, CH_4 and

C_2H_4 and increased the yield of CO_2. However, the B:S showed no obvious effect on the yield of C_2H_6. Similar results were reported by Sadaka et al. [26] for steam gasification of wheat straw.

6.3 HHV of Syngas

When the FV was increased from 0.35 to 0.45 m/s (28.57%), the HHV of syngas decreased from 9.08 to 7.19 MJ/Nm^3 (26.29%), from 9.25 to 7.30 MJ/Nm^3 (26.71%), from 9.63 to 7.62 MJ/Nm^3 (26.38%) at the SFR of 0.20 kg/min and the B:S of 3.00, 4.00 and 5.00 kg/kg; from 9.22 to 7.72 MJ/Nm^3 (19.43%), from 9.54 to 7.95 MJ/Nm^3 (20.00%), from 9.94 to 8.00 MJ/Nm^3 (24.25%) at the SFR of 0.25 kg/min and the B:S of 3.00, 4.00 and of 5.00 kg/kg; and from 9.07 to 7.66 MJ/Nm^3 (18.41%), from 9.69 to 7.87 MJ/Nm^3 (23.13%) and from 10.10 to 8.09 MJ/Nm^3 (24.85%) MJ/Nm^3 the SFR of 0.30 kg/min and the B:S of 3.00, 4.00 and 5.00 kg/kg, respectively. Sharma et al. [24] stated that higher FV can breakdown segregated lumps and remove in-bed channels, resulting in a better particle mixing and consequently a higher HHV of syngas.

The results showed that when the SFR was increased from 0.20 to 0.30 kg/min (50.00%), the HHV of syngas fluctuated between 9.07 and 9.22 MJ/Nm^3, between 9.25 and 9.69 MJ/Nm^3, between 9.63 and 10.10 MJ/Nm^3 at the FV of 0.35 m/s and the B:S of 3.00, 4.00 and 5.00 kg/kg; between 8.01 and 8.15 MJ/Nm^3, between 8.32 and 8.60 MJ/Nm^3, between 8.53 and 8.78 MJ/Nm^3 at the FV of 0.40 m/s and the B:S of 3.00, 4.00 and B:S of 5.00 kg/kg; and between 7.19 and 7.72 MJ/Nm^3, between 7.30 and 7.95 MJ/Nm^3 and between 7.62 and 8.09 MJ/Nm^3 at the FV of 0.45 m/s and the B:S of 3.00, 4.00 and 5.00 kg/kg, respectively. The SFR of 0.25 MJ/Nm^3 produced higher HHV than the SFRs of 0.20 and 0.30 MJ/Nm^3. Kaewpanha et al. [28] stated that tar steam reforming and water–gas shift reactions could be promoted by the flow rate of steam (SFR) thereby increasing the HHV of syngas. However, Karatas et al. [29] reported that the quality (HHV) of syngas was nearly constant when steam amount increased.

However, when the B:S was increased from 3.00 to 5.00 kg/kg (66.67%), the HHV of syngas increased from 9.08 to 9.63 (6.06%), from 9.22 to 9.94 (7.81%), from 9.07 to 10.10 (11.36%) at at the FV of 0.35 m/s and the SFR of 0.20, 0.25 and 0.30 kg/min; from 8.01 to 8.53 (6.49%), from 8.15 to 8.78 (7.73%), from 8.01 to 8.57 (6.99%) at the FV of 0.40 m/s and the SFR of 0.20, 0.25 and 0.30 kg/min; and from 7.19 to 7.62 (5.98%), from 7.72 to 8.00 (3.63%), and from 7.66 to 8.09 (5.61%) MJ/Nm^3 at the FV of 0.45 m/s and the SFR of 0.20, 0.25 and 0.30 kg/min, respectively. Sadaka et al. [26] stated the pyrolysis process and cracking of the hydrocarbons caused by increased B:S could increase the mole fractions of the combustible gases (CH_4, H_2 and CO) and thereby increasing the HHV of syngas. The results obtained from this study showed that the effect of FV on the HHV of syngas (18.41-26.71%) was the highest, followed by the effect of B:S (3.63-11.36%) and the SFR (1.65-8.90%).

6.4 Energy Values of Syngas

The energy values of gas components at various FVs, SFRs and B:Ss are shown in Table 7. The detailed distributions are shown in Table 8. The effects of FV, SFR and B:S on the total energy of syngas are show in Figs. 6-8.

The energy values of CO, H_2, N_2, CO_2, CH_4, C_2H_4 and C_2H_6 varied within the ranges of 1627.09-4646.60, 1543.30-2896.11, 274.75-1742.86, 82.03-574.24, 3225.39-4931.40, 1493.35-3777.44 and 892.74-2319.72 kJ/kg fuel, respectively. Although different gas components contributed differently to the total energy of syngas, the overall distribution of (CH_4 & CO & C_2H_4 & H_2)>C_2H_6>(N_2 & CO_2) was observed. Zhang et al. (2011) stated that the energy value of gas component is determined by the temperature of the bed and the yield of the gas component. Equation (3) shows that both the increases in enthalpy and yield can result in increases in the physical energy of gas component. Also, equation (6) shows that the increase in yield can lead to increases in the chemical energy of gas component.

When the FV was increased from 0.35 to 0.45 (28.57%), the total energy of syngas varied from 18186.38 to 20004.54 (10.00%), from 16184.70 to 17241.61 (6.53%), from 15327.66 to 15727.10 (2.61%) at the SFR of 0.20 kg/min and the B:S of 3.00, 4.00 and 5.00 kg/kg; from 15642.60-16889.49 (7.97%), 14832.82-15151.60 (2.15%), 13823.74-13984.13 (1.16%) at the SFR of 0.25 kg/min and the B:S of 3.00, 4.00 and 5.00 kg/kg; and 12181.91 to 14922.04 (22.49%), from 10508.71 to 13199.91 (25.61%) and from 9612.65 to 12360.99 (28.59%) kJ/kg fuel at the SFR of 0.30 kg/min and the B:S of 3.00, 4.00 and 5.00 kg/kg, respectively. Sharma et al. [24] stated that higher FV can result in a better particle mixing and consequently higher quality of syngas.

Table 7. Energy values of gas components

FV	SFR	B:S	Energy values (kJ/kg)						
(m/s)	(kg/min)	(kg/kg)	CO	H_2	N_2	CO_2	CH_4	C_2H_4	C_2H_6
0.35	0.20	3.00	4382.82	2579.32	1154.87	82.03	4594.69	3394.56	1998.10
		4.00	3917.69	2356.87	842.49	208.10	4034.44	3070.49	1754.61
		5.00	3639.06	2156.20	632.74	279.52	3818.13	3030.65	1771.36
	0.25	3.00	3282.14	2212.99	795.33	322.46	4931.40	2573.19	1525.10
		4.00	3141.94	2141.62	546.88	439.87	4701.02	2454.46	1407.04
		5.00	2891.32	2006.76	418.07	416.98	4241.54	2501.82	1507.64
	0.30	3.00	2525.16	1994.01	547.78	355.87	4590.80	2022.33	1164.72
		4.00	2003.31	1805.20	344.61	305.23	3855.80	1569.08	903.06
		5.00	1731.87	1543.30	274.75	259.09	3339.94	1531.72	931.98
0.40	0.20	3.00	4536.66	2775.36	1453.21	93.18	4681.24	3658.05	2101.11
		4.00	4126.64	2335.98	1048.29	216.11	4276.48	3141.72	1916.01
		5.00	3844.58	2119.74	796.00	281.65	3965.11	2920.74	1724.42
	0.25	3.00	3526.62	2442.19	1002.74	332.29	4681.48	2808.01	1673.20
		4.00	3303.23	2328.97	693.07	439.78	4422.54	2484.54	1479.47
		5.00	3013.60	2106.66	553.25	462.96	4072.66	2311.66	1328.44
	0.30	3.00	2044.95	1910.54	747.62	312.19	4039.13	1956.44	1171.04
		4.00	1810.82	1971.40	504.03	330.04	3395.55	1582.66	914.21
		5.00	1627.09	1748.58	375.91	317.17	3225.39	1493.35	892.74
0.45	0.20	3.00	4646.60	2896.11	1742.86	453.71	4168.10	3777.44	2319.72
		4.00	3961.01	2426.52	1314.82	277.16	3885.73	3373.94	2002.45
		5.00	3516.59	2206.73	1123.71	337.70	3688.53	3083.89	1769.94
	0.25	3.00	3703.98	2557.98	1310.92	307.39	4757.17	2693.26	1558.80
		4.00	3189.13	2309.33	960.37	442.93	4253.16	2401.75	1438.48
		5.00	2828.11	2164.80	710.19	491.63	4085.89	2216.40	1326.73
	0.30	3.00	3177.11	2436.92	910.77	481.88	4675.38	2047.24	1192.74
		4.00	2272.71	2501.74	708.28	534.96	4224.42	1841.52	1116.27
		5.00	2077.17	2338.73	520.13	574.24	4044.37	1776.70	1029.66

When the SFR was increased from 0.20 kg/min to 0.30 kg/min (50.00%), the total energy of syngas decreased from 18186.38 to 13200.67 (37.77%), from 16184.70 to 10786.29 (50.05%), from 15327.66 to 9612.65 (59.45%), from 19298.82 to 12181.91 (58.42%), from 17061.24 to 10508.71 (62.35%), 9680.22-15652.23 (61.69%), 14922.04-20004.54 (34.06%), 13199.91-17241.61 (30.62%) and from 15727.10 to 12360.99 (27.23%) kJ/kg fuel at the FV of 0.35 m/s and the B:S of 3.00 kg/kg, the FV=0.35 m/s and the B:S of 4.00 kg/kg, the FV of 0.35 m/s and the B:S of 5.00 kg/kg, the FV of 0.40 m/s and the B:S of 3.00 kg/kg, the FV of 0.40 m/s and the B:S of 4.00 kg/kg, the FV of 0.40 m/s and the B:S of 5.00 kg/kg, the FV of 0.45 m/s and the B:S of 3.00 kg/kg, the FV of 0.45 m/s and the B:S of 4.00 kg/kg and the FV of 0.45 m/s and the B:S of 5.00 kg/kg, respectively. Karatas et al. [29] reported that the quality of syngas was nearly constant when steam amount increased.

When the B:S was increased from 3.00 kg/kg to 5.00 kg/kg (66.67%), the total energy of syngas decreased from 18186.38 to 15327.66 (18.65%), from 15642.60 to 13984.13 (11.86%), from 13200.67 to 9612.65 (37.33%), from 19298.82 to 15652.23 (23.30%), from 16466.53 to 13849.24 (18.90%), from 12181.91 to 9680.22 (25.84%), from 20004.54 to 15727.10 (27.20%), from 16889.49 to 13823.74 (22.18%) and from 14922.04 to 12360.99 (20.72%) kJ/kg fuel at the FV of 0.35 m/s and the SFR of 0.20 kg/min, the FV of 0.35 m/s and the SFR of 0.25 kg/min, the FV of 0.35 m/s and the SFR of 0.30 kg/min, the FV of 0.40 m/s and the SFR of 0.20 kg/min, the FV of 0.40 m/s and the SFR of 0.25 kg/min, the FV of 0.40 m/s and the SFR of 0.30 kg/min; FV=0.45 m/s and SFR=0.20 kg/min, FV=0.45 m/s and SFR=0.25 kg/min, and FV=0.45 m/s and the SFR of 0.30 kg/min, respectively. Sadaka et al. (2002) stated that increase in B/S could increase the quality of syngas. However, the results obtained from this study showed that the effect of SFR on the total energy of syngas (27.23-62.35%) was the highest, followed by the B:S (11.86-37.33%) and the FV (1.16-28.59%).

Table 8. Energy distribution of syngas

FV (m/s)	SFR (kg/min)	B/S (kg/kg)	Energy distribution
0.35	0.20	3.00	$CH_4>CO>C_2H_4>H_2>C_2H_6>N_2>CO_2$
		4.00	$CH_4>CO>C_2H_4>H_2>C_2H_6>N_2>CO_2$
		5.00	$CH_4>CO>C_2H_4>H_2>C_2H_6>N_2>CO_2$
	0.25	3.00	$CH_4>CO>C_2H_4>H_2>C_2H_6>N_2>CO_2$
		4.00	$CH_4>CO>C_2H_4>H_2>C_2H_6>N_2>CO_2$
		5.00	$CH_4>CO>C_2H_4>H_2>C_2H_6>N_2>CO_2$
	0.30	3.00	$CH_4>CO>C_2H_4>H_2>C_2H_6>N_2>CO_2$
		4.00	$CH_4>CO>H_2>C_2H_4>C_2H_6>N_2>CO_2$
		5.00	$CH_4>CO>H_2>C_2H_4>C_2H_6>N_2>CO_2$
0.40	0.20	3.00	$CH_4>CO>C_2H_4>H_2>C_2H_6>N_2>CO_2$
		4.00	$CH_4>CO>C_2H_4>H_2>C_2H_6>N_2>CO_2$
		5.00	$CH_4>CO>C_2H_4>H_2>C_2H_6>N_2>CO_2$
	0.25	3.00	$CH_4>CO>C_2H_4>H_2>C_2H_6>N_2>CO_2$
		4.00	$CH_4>CO>C_2H_4>H_2>C_2H_6>N_2>CO_2$
		5.00	$CH_4>CO>C_2H_4>H_2>C_2H_6>N_2>CO_2$
	0.30	3.00	$CH_4>CO>C_2H_4>H_2>C_2H_6>N_2>CO_2$
		4.00	$CH_4>CO>H_2>C_2H_4>C_2H_6>N_2>CO_2$
		5.00	$CH_4>H_2>CO>C_2H_4>C_2H_6>N_2>CO_2$
0.45	0.20	3.00	$CO>CH_4>C_2H_4>H_2>C_2H_6>N_2>CO_2$
		4.00	$CO>CH_4>C_2H_4>H_2>C_2H_6>N_2>CO_2$
		5.00	$CH_4>CO>C_2H_4>H_2>C_2H_6>N_2>CO_2$
	0.25	3.00	$CH_4>CO>C_2H_4>H_2>C_2H_6>N_2>CO_2$
		4.00	$CH_4>CO>C_2H_4>H_2>C_2H_6>N_2>CO_2$
		5.00	$CH_4>CO>C_2H_4>H_2>C_2H_6>N_2>CO_2$
	0.30	3.00	$CH_4>CO>H_2>C_2H_4>C_2H_6>N_2>CO_2$
		4.00	$CH_4>H_2>CO>C_2H_4>C_2H_6>N_2>CO_2$
		5.00	$CH_4>H_2>CO>C_2H_4>C_2H_6>CO_2>N_2$

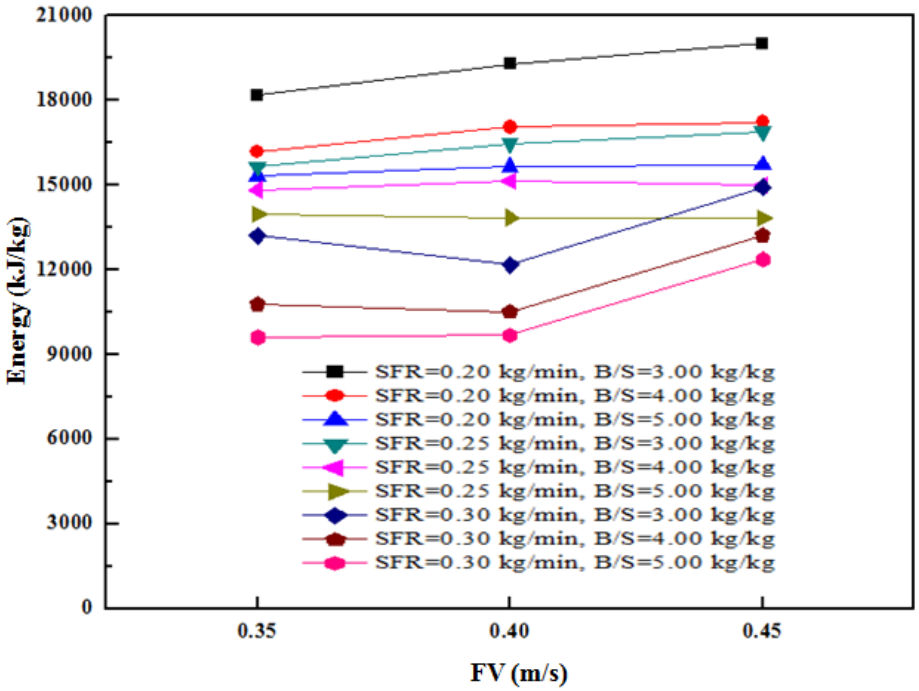

Fig. 6. Effect of FV on the energy value of the syngas

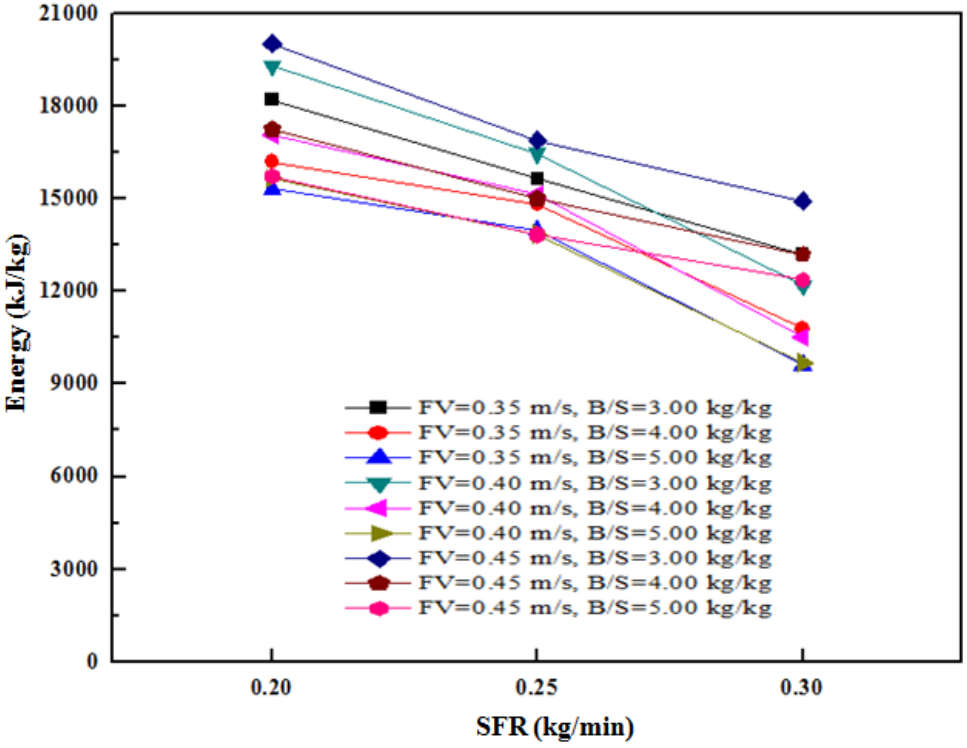

Fig. 7. Effect of SFR on the energy value of the syngas

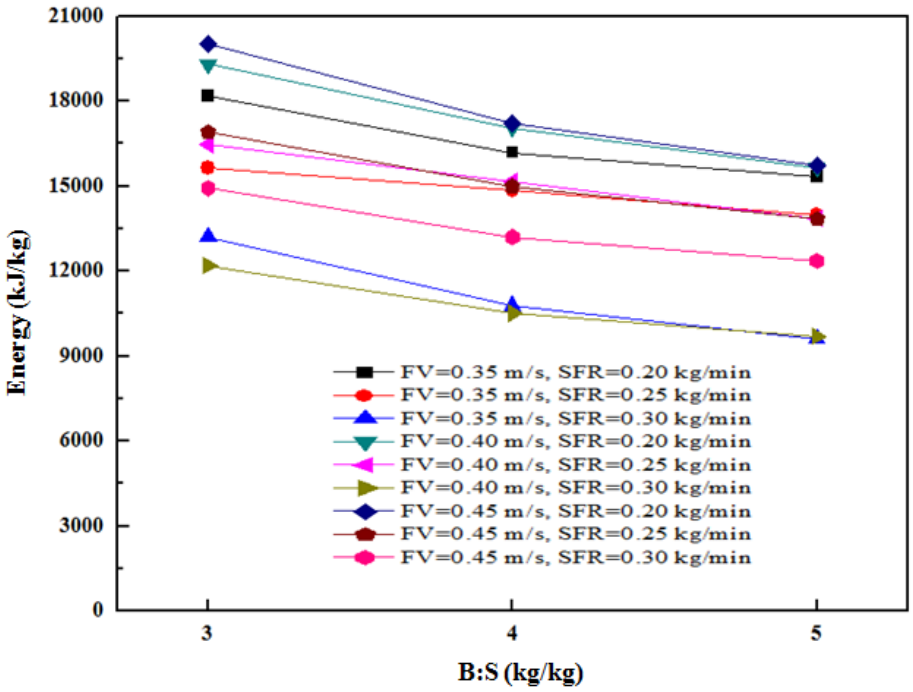

Fig. 8. Effect of B:S on the energy value of the syngas

6.5 Exergy Values of Syngas

Table 9 shows the exergy values of gas components at various FVs, SFRs and B:Ss. The detailed distributions are shown in Table 10. The effects of FV, SFR and B/S on the total exergy of syngas are shown in Figs. 9-11.

The exergy values of CO, H_2, N_2, CO_2, CH_4, C_2H_4 and C_2H_6 varied within the ranges of 1486.70-4224.40, 1183.82-2209.00, 60.26-677.26, 54.02-452.97, 2913.74-4448.38, 1404.76-3541.76 and 833.00-2156.42 kJ/kg fuel, respectively. Although different gas components contributed differently to the total exergy of syngas, the overall distribution of (CH_4 & CO)>(C_2H_4 & H_2 & C_2H_6)>(N_2 &CO_2) was observed. Zhang et al. [21] stated that the exergy values were determined by the temperature of the bed and the yield of the gas component. Equation (9) shows that the increases in enthalpy and entropy can result in increases in the physical exergy of gas component, while the increase in the yield of gas component can lead to increases in the physical exergy. Also, equation (11) shows that increases in the yield of gas component can result in increases in its chemical exergy.

When the FV was increased from 0.35 to 0.45 (28.57%), the total exergy of syngas varied from 15610.94 to 16886.06 (8.17%), from 13953.45 to 14662.82 (5.08%), from 13313.19 to 13506.73 (1.45%), from 13465.84 to 14294.30 (6.15%), from 12759.57 to 13038.48 (2.19%), from 11833.33 to 12205.80 (3.15%), from 10374.92 to 12669.38 (22.12%), from 8968.59 to 11200.96 (24.89%) and from 8323.20 to 10564.64 (26.93%) kJ/kg fuel at the SFR of 0.20 kg/min and the B:S of 3.00 kg/kg, the SFR of 0.20 kg/min and the B:S of 4.00 kg/kg, the SFR of 0.20 kg/min and the B:S of 5.00 kg/kg, the SFR of 0.25 kg/min and the B:S of 3.00 kg/kg, the SFR of 0.25 kg/min and the B:S of 4.00 kg/kg, the SFR of 0.25 kg/min and the B:S of 5.00 kg/kg, the SFR of 0.30 kg/min and the B:S of 3.00 kg/kg, the SFR of 0.30 kg/min and the B:S of 4.00 kg/kg and the SFR of 0.30 kg/min and the B:S of 5.00 kg/kg, respectively.

Table 9. Exergy values of gas components

FV	SFR	B:S	Exergy values (kJ/kg fuel)						
(m/s)	(kg/min)	(kg/kg)	CO	H_2	N_2	CO_2	CH_4	C_2H_4	C_2H_6
0.35	0.20	3.00	3992.02	1971.09	406.20	54.02	4139.08	3187.91	1860.62
		4.00	3572.80	1802.46	269.35	149.53	3637.62	2886.20	1635.49
		5.00	3322.92	1649.82	180.87	208.93	3446.06	2851.61	1652.99
	0.25	3.00	2992.36	1691.58	255.21	239.73	4448.38	2417.62	1420.97
		4.00	2867.91	1638.44	152.94	339.92	4244.48	2308.03	1312.17
		5.00	2642.68	1536.66	102.50	327.85	3833.17	2355.16	1407.79
	0.30	3.00	2304.75	1525.23	156.41	271.52	4145.14	1901.11	1085.89
		4.00	1831.58	1383.93	83.37	238.70	3486.42	1476.69	843.01
		5.00	1585.18	1183.82	60.26	205.29	3022.42	1442.92	870.99
0.40	0.20	3.00	4125.57	2118.18	550.60	61.40	4210.34	3430.91	1953.64
		4.00	3757.07	1782.87	366.31	153.13	3850.26	2949.09	1783.40
		5.00	3504.75	1618.49	252.88	206.14	3573.51	2744.25	1606.70
	0.25	3.00	3209.84	1864.86	352.19	242.79	4215.23	2634.81	1556.70
		4.00	3010.22	1780.31	217.71	332.73	3986.39	2333.31	1377.82
		5.00	2748.89	1610.94	160.62	356.87	3673.77	2172.50	1238.09
	0.30	3.00	1863.35	1459.91	250.04	233.01	3641.29	1836.96	1090.36
		4.00	1652.35	1510.23	149.29	253.10	3064.19	1487.35	852.07
		5.00	1486.70	1339.91	97.67	247.42	2913.74	1404.76	833.00
0.45	0.20	3.00	4224.40	2209.00	677.26	331.50	3745.72	3541.76	2156.42
		4.00	3602.29	1850.34	492.21	197.99	3493.60	3164.39	1861.99
		5.00	3202.19	1683.63	397.32	247.61	3320.07	2895.15	1647.50
	0.25	3.00	3367.50	1952.39	500.38	221.66	4279.17	2524.59	1448.61
		4.00	2902.60	1763.87	340.35	331.96	3829.36	2253.28	1338.15
		5.00	2576.61	1654.14	229.26	375.40	3681.87	2080.86	1235.20
	0.30	3.00	2891.85	1861.35	314.77	362.02	4210.20	1920.03	1109.18
		4.00	2071.96	1915.15	222.61	413.48	3809.07	1729.16	1039.54
		5.00	1895.68	1791.21	145.70	452.97	3649.82	1669.62	959.65

Table 10. Exergy distribution of syngas

FV (m/s)	SFR (kg/min)	B:S (kg/kg)	Exergy Distribution
0.35	0.20	3.00	$CH_4>CO>C_2H_4>H_2>C_2H_6>N_2>CO_2$
		4.00	$CH_4>CO>C_2H_4>H_2>C_2H_6>N_2>CO_2$
		5.00	$CH_4>CO>C_2H_4>C_2H_6>H_2>CO_2>N_2$
	0.25	3.00	$CH_4>CO>C_2H_4>H_2>C_2H_6>N_2>CO_2$
		4.00	$CH_4>CO>C_2H_4>H_2>C_2H_6>CO_2>N_2$
		5.00	$CH_4>CO>C_2H_4>H_2>C_2H_6>CO_2>N_2$
	0.30	3.00	$CH_4>CO>C_2H_4>H_2>C_2H_6>CO_2>N_2$
		4.00	$CH_4>CO>C_2H_4>H_2>C_2H_6>CO_2>N_2$
		5.00	$CH_4>CO>C_2H_4>H_2>C_2H_6>CO_2>N_2$
0.40	0.20	3.00	$CH_4>CO>C_2H_4>H_2>C_2H_6>N_2>CO_2$
		4.00	$CH_4>CO>C_2H_4>C_2H_6>H_2>N_2>CO_2$
		5.00	$CH_4>CO>C_2H_4>H_2>C_2H_6>N_2>CO_2$
	0.25	3.00	$CH_4>CO>C_2H_4>H_2>C_2H_6>N_2>CO_2$
		4.00	$CH_4>CO>C_2H_4>H_2>C_2H_6>CO_2>N_2$
		5.00	$CH_4>CO>C_2H_4>H_2>C_2H_6>CO_2>N_2$
	0.30	3.00	$CH_4>CO>C_2H_4>H_2>C_2H_6>N_2>CO_2$
		4.00	$CH_4>CO>H_2>C_2H_4>C_2H_6>CO_2>N_2$
		5.00	$CH_4>CO>C_2H_4>H_2>C_2H_6>CO_2>N_2$
0.45	0.20	3.00	$CO>CH_4>C_2H_4>H_2>C_2H_6>N_2>CO_2$
		4.00	$CO>CH_4>C_2H_4>C_2H_6>H_2>N_2>CO_2$
		5.00	$CH_4>CO>C_2H_4>H_2>C_2H_6>N_2>CO_2$
	0.25	3.00	$CH_4>CO>C_2H_4>H_2>C_2H_6>N_2>CO_2$
		4.00	$CH_4>CO>C_2H_4>H_2>C_2H_6>N_2>CO_2$
		5.00	$CH_4>CO>C_2H_4>H_2>C_2H_6>CO_2>N_2$
	0.30	3.00	$CH_4>CO>C_2H_4>H_2>C_2H_6>CO_2>N_2$
		4.00	$CH_4>CO>H_2>C_2H_4>C_2H_6>CO_2>N_2$
		5.00	$CH_4>CO>H_2>C_2H_4>C_2H_6>CO_2>N_2$

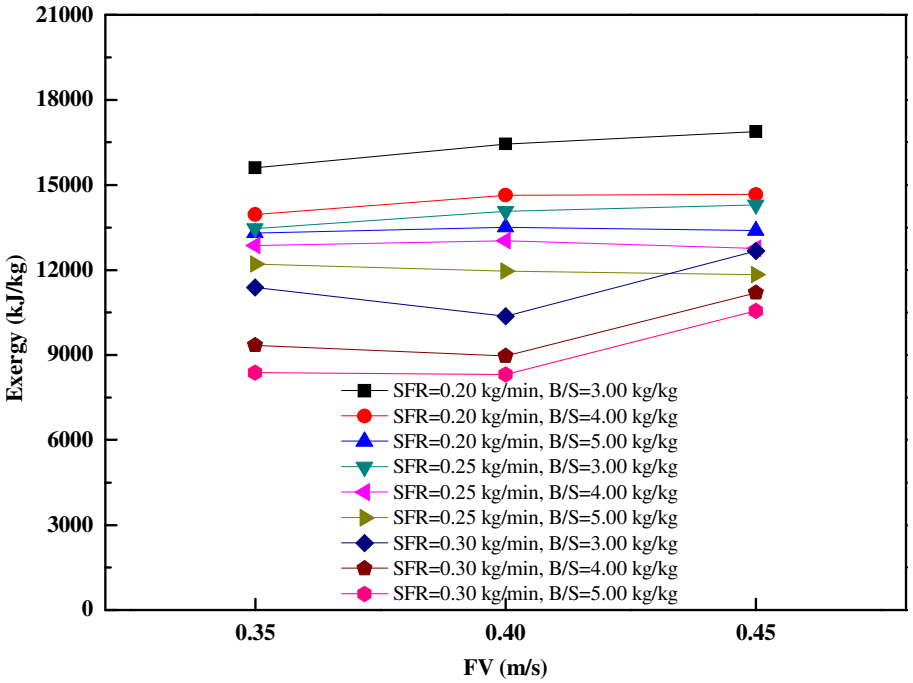

Fig. 9. Effect of FV on the exergy value of the syngas

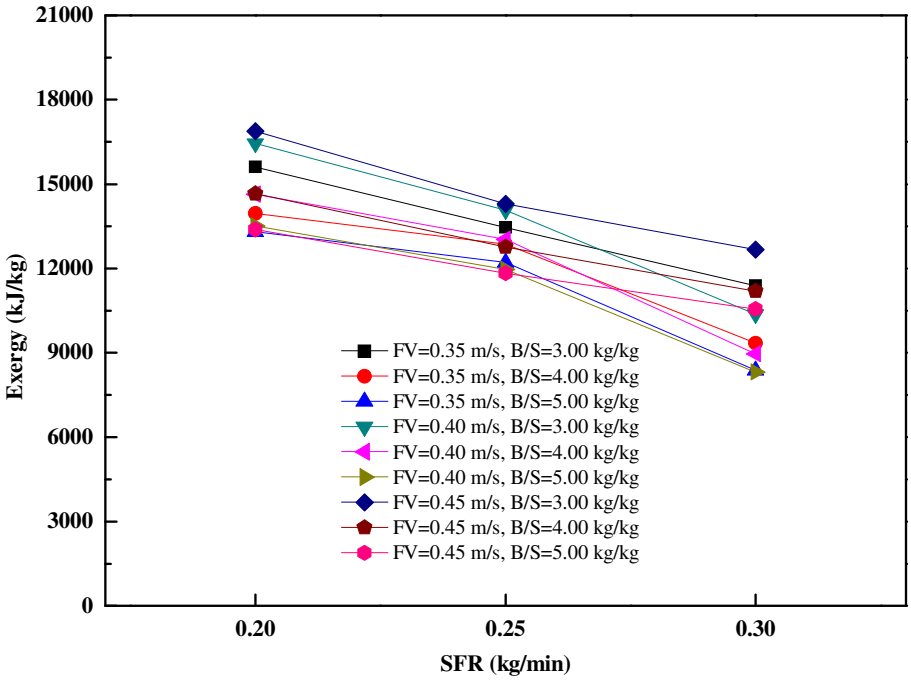

Fig. 10. Effect of SFR on the exergy value of the syngas

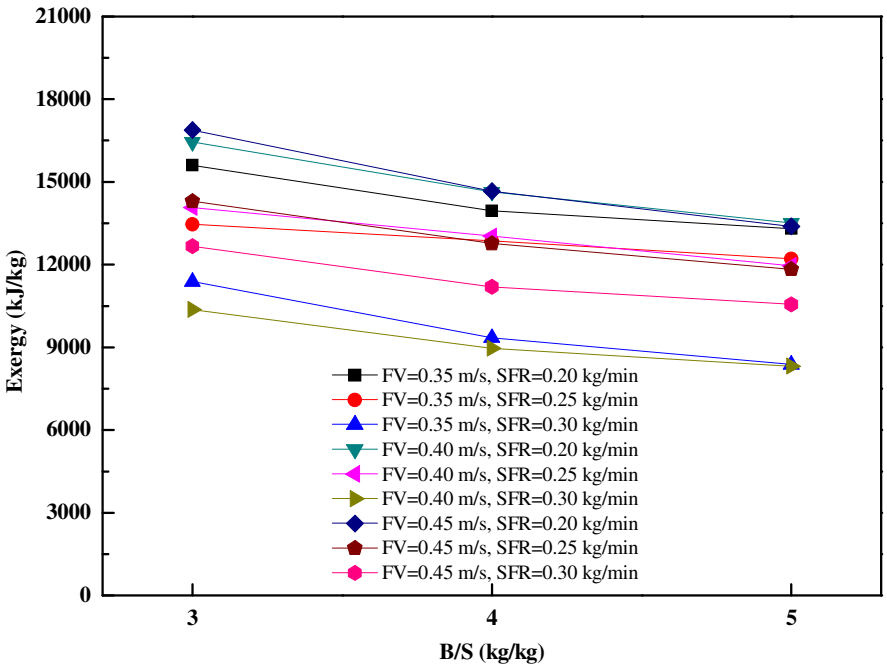

Fig. 11. Effect of B:S on the exergy value of the syngas

When the SFR was increased from 0.20 kg/min to 0.30 kg/min (50.00%), the total exergy of syngas decreased from 15610.94 to 11390.05 (37.06%), from 13953.45 to 9343.71 (49.34%), from 13313.19 to 8370.88 (59.04%), from 16450.64 to 10374.92 (58.56%), from 14642.12 to 8968.59 (63.26%), from 13506.73 to 8323.20 (62.28%), from 16886.06 to 12669.38 (33.28%),

from 14662.82 to 11200.96 (30.91%) and from 13393.47 to 10564.64 (26.78%) kJ/kg fuel at the FV of 0.35 m/s and the B:S of 3.00 kg/kg, the FV of 0.35 m/s and the B:S of 4.00 kg/kg, the FV of 0.35 m/s and the B:S of 5.00 kg/kg, the FV of 0.40 m/s and the B:S of 3.00 kg/kg, the FV of 0.40 m/s and the B:S of 4.00 kg/kg, the FV of 0.40 m/s and the B:S of 5.00 kg/kg, the FV of 0.45 m/s and the B:S of 3.00 kg/kg, the FV of 0.45 m/s and the B:S of 4.00 kg/kg and the FV of 0.45 m/s and the B:S of 5.00 kg/kg, respectively.

When the B:S was increased from 3.00 kg/kg to 5.00 kg/kg (66.67%), the total exergy of syngas decreased from 15610.94to 13313.19 (17.26%), from 13465.84 to 12205.80 (10.32%), from 11390.05 to 8370.88 (36.07%), from 16450.64 to 13506.73 (21.80%), from 14076.42 to 11961.68 (17.68%), from 10374.92 to 8323.20 (24.65%), from 16886.06 to 13393.47 (26.08%), from 14294.30 to 11833.33 (20.80%) and from 12669.38 to 10564.64 (19.92%) kJ/kg fuel at the FV of 0.35 m/s and the SFR of 0.20 kg/min, the FV of 0.35 m/s and the SFR of 0.25 kg/min, the FV of 0.35 m/s and the SFR of 0.30 kg/min, the FV of 0.40 m/s and the SFR of 0.20 kg/min, the FV of 0.40 m/s and the SFR of 0.25 kg/min, the FV of 0.40 m/s and the SFR of 0.30 kg/min; the FV of 0.45 m/s and the SFR of 0.20 kg/min, the FV of 0.45 m/s and the SFR of 0.25 kg/min and the FV of 0.45 m/s and the SFR of 0.30 kg/min, respectively.

The results obtained from this study showed that the effect of SFR on the total exergy of syngas (26.78-63.26%) was the highest, followed by B:S (10.32-36.07%) and FV (1.45-26.93%). Prins et al. [30] and Zhang et al. [14] stated that the exergy values of the gas components were lower than their corresponding energy values due to: (a) the physical exergy of a gas component is lower than the corresponding physical energy and (b) the chemical exergy values of combustible gases are lower than the corresponding chemical energy values. Similar results were reported for the exergy of syngas by Karamarkovic and Karamarkovic [31] from a biomass represented by $CH_{1.4}O_{0.59}N_{0.0017}$ and by Sreejith et al. [32] for coconut shell, coir pith, bamboo and eucalyptus.

7. CONCLUSIONS

The energy and exergy of syngas from the air-steam gasification of wheat straw in a dual-distributor fluidized bed gasifier were evaluated at various FVs, SFRs and B/Ss. The energy values of CO, H_2, N_2, CO_2, CH_4, C_2H_4 and C_2H_6 varied within the ranges of 1627.09-4646.60, 1543.30-2896.11, 274.75-1742.86, 82.03-574.24, 3225.39-4931.40, 1493.35-3777.44 and 892.74-2319.72 kJ/kg fuel, respectively. The overall energy distribution was (CH_4 & CO & C_2H_4 & H_2)>C_2H_6>(N_2 & CO_2). The results showed that when the FV was increased from 0.35 to 0.45 (28.57%), the total energy of syngas fluctuated by 1.16-28.59% depending on the SFR and B/S used. Increasing the SFR from 0.20 kg/min to 0.30 kg/min (50.00%), decreased the total energy of syngas by 27.23-62.35% depending on the FV and B/S used. Increasing the B/S from 3.00 kg/kg to 5.00 kg/kg (66.67%), decreased the total energy of syngas by 11.86-37.33% depending on the FV and SFR used. The effect of SFR on the total energy of syngas was the highest, followed by B/S and FV. The exergy values of CO, H_2, N_2, CO_2, CH_4, C_2H_4 and C_2H_6 varied within the ranges of 1486.70-4224.40, 1183.82-2209.00, 60.26-677.26, 54.02-452.97, 2913.74-4448.38, 1404.76-3541.76 and 833.00-2156.42 kJ/kg fuel, respectively. The overall exergy distribution was (CH_4 & CO)>(C_2H_4 & H_2 & C_2H_6)>(N_2 &CO_2). When the FV was increased from 0.35 to 0.45 (28.57%), the total exergy of syngas fluctuated by 1.45-26.93% depending on the SFR and B/S used. Increasing the SFR from 0.20 kg/min to 0.30 kg/min (50.00%), decreased the total exergy of syngas by 26.78-63.26% depending on the FV and B/S used. Increasing the B/S from 3.00 kg/kg to 5.00 kg/kg (66.67%), decreased the total exergy of syngas by 10.32-36.07% depending on the FV and SFR used. The effect of SFR on the total exergy of syngas was the highest, followed by B/S and FV. The results showed that the exergy values of the syngas were lower than their energy values because the gas components contributed differently to the energy and exergy (the physical exergy of gas components are lower than the corresponding physical energy and the chemical exergy of combustible gases are lower than the corresponding chemical energy). The highest energy (20004.54 kJ/kg fuel) and exergy (16886.06 kJ/kg fuel) of syngas were obtained at the FV of 0.45 m/s, SFR of 0.20 kg/min and B/S of 3.00 kg/kg.

ACKNOWLEDGEMENTS

The project was funded by National Science and Engineering Council (NSERC) of Canada and China Postdoctoral Science Foundation.

COMPETING INTERESTS

Authors have declared that no competing interests exist.

REFERENCES

1. Saidur R, Abdelaziz EA, Demirbas A, Hossain MS, Mekhilef S. A review on biomass as a fuel for boilers. Renewable and Sustainable Energy Reviews. 2011;15 (5):2262–2289.
   DOI: 10.1016/j.rser.2011.02.015
2. Heidenreich S, Foscolo PU. New concepts in biomass gasification. Progress in Energy and Combustion Science. 2015;46(1):72-95.
   DOI: 10.1016/j.pecs.2014.06.002
3. Parthasarathy P, Narayanan KS. Hydrogen production from steam gasification of biomass: Influence of process parameters on hydrogen yield-A review. Renewable Energy. 2014;66:570–579.
   DOI: 10.1016/j.renene.2013.12.025
4. Balat H, Kırtay E. Hydrogen from biomass - Present scenario and future prospects. International Journal of Hydrogen Energy. 2010;35(14):7416–7426.
   DOI: 10.1016/j.ijhydene.2010.04.137
5. Ruiz JA, Juarez MC, Morales MP, Muñoz P and Mendivil, MA. Biomass gasification for electricity generation: Review of current technology barriers. Renewable and Sustainable Energy Reviews. 2013;18: 174–183.
   DOI: 10.1016/j.rser.2012.10.021
6. Materazzi M, Lettieri P, Mazzei L, Taylor R and Chapman C. Thermodynamic modelling and evaluation of a two-stage thermal process for waste gasification. Fuel. 2013;108:356–369.
   DOI: 10.1016/j.fuel.2013.02.037
7. Miguel GS, Domínguez MP. Hernández M and Sanz-Pérez F. Characterization and potential applications of solid particles produced at a biomass gasification plant. Biomass and Bioenergy. 2012;47:134–144.
   DOI.10.1016/j.biombioe.2012.09.049
8. Nipattummakul N, Ahmed I, Kerdsuwan S, Gupta AK. Hydrogen and syngas production from sewage sludge via steam gasification. International Journal of Hydrogen Energy. 2010;35(21):11738–11745.
   DOI: 10.1016/j.ijhydene.2010.08.032
9. Franco C, Pinto F, Gulyurtlu I, Cabrita I. The study of reactions influencing the biomass steam gasification process. Fuel. 2003;82(7):835–842.
   DOI: 10.1016/S0016-2361(02)00313-7
10. Umeki K, Son Y, Namioka T, Yoshikawa K. Basic studies on hydrogen-rich gas production by high temperature steam gasification of solid wastes. Journal of Environment and Engineering. 2009;4: 211–221.
    DOI: 10.1299/jee.4.211
11. Wei L, Xu S, Zhang L, Liu C, Zhu H, Liu S. Steam gasification of biomass for hydrogen-rich gas in a free-fall reactor. International Journal of Hydrogen Energy. 2007;32(1):24–31.
    DOI: 10.1016/j.ijhydene.2006.06.002
12. Dincer I, Cengel YA. Energy, entropy and exergy concepts and their role in thermal engineering. Entropy. 2001;3(3):116-149.
    DOI: 10.3390/e3030116
13. Bastianoni S, Fachini A, Susani L, Tiezzi E. Energy as a function of exergy. Energy. 2007;32(7):1158-1162.
    DOI: 10.1016/energy/2006.08.009
14. Zhang Y, Li B, Li H, Liu H. Thermodynamic evaluation of biomass gasification with air in autothermal gasifiers. Thermochimica Acta. 2011;519(1-2):65–71.
    DOI:10.1016/j.tca.2011.03.005
15. Zhang Y. Thermodynamic study on gasification process of biomass fuels. Dissertation for the doctoral degree in engineering. Harbin Institute of Technology, Harbin, China; 2012.
16. Loha C, Chattopadhyay H, Chatterjee PK. Thermodynamic analysis of hydrogen rich synthetic gas generation from fluidized bed gasification of rice husk. Energy. 2011;36: 4063–4071.
    DOI: 10.1016/j.energy.2011.04.042
17. Lu Y, Guo L, Zhang X, Yan Q. Thermodynamic modeling and analysis of biomass gasification for hydrogen production in supercritical water. Chemical Engineering Journal. 2007;131:233–244.
    DOI: 10.1016/j.cej.2006.11.016
18. Cengel YA, Boles MA. Thermodynamics: an engineering approach (fifth edition). New York, McGraw-Hill, Inc; 2006.
19. Moran MJ, Shapiro HN, Boettner DD, Bailey MB. Fundamentals of engineering thermodynamics (seventh edition). John Wiley & Sons, Inc; 2011.
20. Al-Weshahi MA, Anderson A, Tian G. Exergy efficiency enhancement of MSF desalination by heat recovery from hot distillate water stages. Applied Thermal Engineering. 2013;53:226–233.
    DOI:10.1016/j.applthermaleng.2012.02.013
21. Zhang Y, Li B, Li H, Zhang B. Exergy analysis of biomass utilization via steam

gasification and partial oxidation. Thermochimica Acta. 2012;538:21–28. DOI:10.1016/j.tca.2012.03.013

22. Ghaly AE, A. Ergudenler A, Al Suhaibani A, Ramakrishnan V. Development and evaluation of straw chopping system for fluidized bed gasifier. The International Journal of Engineering and Science. 2013; 2(11):97-110.
23. Ghaly AE, Ergudenler A, Al Suhaibani A, V Ramakrishnan V. Development and evaluation of a low density biomass feeding system for fluidized bed gasifer. The International Journal of Engineering and Science. 2013;6(3):327-339.
24. Sharma AM, Kumar A, Patil KN, Huhnke RL. Fluidization characteristics of a mixture of gasifier solid residues, switchgrass and inert material. Powder Technology. 2013; 235:661–668. DOI: 10.1016/j.powtec.2012.11.025
25. Mansaray K, Ghaly AE, Al-Taweel AM, Hamdullahpur F, Ugursal VI. Air gasification of rice husk in a dual distributor type fluidized bed gasifier. Biomass and Bioenergy. 1999;17:315–332. PII: S0961-9534(99)00046-X
26. Sadaka SS, Ghaly AE, Sabbah MA. Two phase biomass air-steam gasification model for fluidized bed reactors: Part II—model sensitivity. Biomass and Bioenergy. 2002;22:463–477. PII: S0961-9534(02)00024-7
27. Li W, Li Q, Chen R, Wu Y, Zhang Y. Investigation of hydrogen production using wood pellets gasification with steam at high temperature over 800°C to 1435°C. International Journal of Hydrogen Energy. 2014;39(11):5580–5588. DOI: 10.1016/j.ijhydene.2014.01.102
28. Kaewpanha M, Guan G, Hao X, Wang Z, Kasai Y, Kusakabe K, Abudula A. Steam co-gasification of brown seaweed and land-based biomass. Fuel Processing Technology. 2014;120:106–112. DOI: 10.1016/j.fuproc.2013.12.013
29. Prins MJ, Ptasinski KJ, Janssen FJG. Thermodynamics of gas-char reactions: First and second law analysis. Chemical Engineering Science. 2003;58:1003–1011. DOI:10.1016/S0009-2509(02)00641-3
30. Karatas H, Olgun H, Akgun F. Experimental results of gasification of waste tire with air & CO2, air & steam and steam in a bubbling fluidized bed gasifier. Fuel Processing Technology. 2012;102: 166–174. DOI: 10.1016/j.fuproc.2012.04.013
31. Karamarkovic R, Karamarkovic V. Energy and exergy analysis of biomass gasification at different temperatures. Energy. 2010;35:537–549. DOI:10.1016/j.energy.2009.10.022
32. Sreejith CC, Muraleedharan C, Arun P. Energy and exergy analysis of steam gasification of biomass materials: A comparative study. International Journal of Ambient Energy. 2013;34(1):35–52. DOI:10.1080/01430750.2012.711085

Peer-review history:
The peer review history for this paper can be accessed here:
http://www.sdiarticle3.com/review-history/49702